Korean J. Chem. Eng., 39(5), 1277-1286 (2022)
DOI: 10.1007/s11814-021-1054-3

pISSN: 0256-1115
eISSN: 1975-7220

High throughput comparative assessment of biofilm formation of *Candida glabrata* on polystyrene material

Bindu Sadanandan*,†, Priya Ashrit*, Lokesh Kyathsandra Nataraj*, Kalidas Shetty, Amruta Puroshottam Jogalekar*, Vijayalakshmi Vaniyamparambath*, and Beena Hemanth*****

*Department of Biotechnology, M S Ramaiah Institute of Technology, Bengaluru, India
**Department of Plant Science, North Dakota State University, Fargo, ND58105, USA
***Department of Microbiology, M S Ramaiah Medical College and Teaching Hospital, Bengaluru, India
(*Received 8 July 2021 • Revised 9 November 2021 • Accepted 26 December 2021*)

Abstract−*Candida glabrata* is the second most reported *Candida* species causing candidiasis next only to *Candida albicans*. Biofilm formation by *C. glabrata* accelerates pathogenicity, so understanding conditions for biofilm formation in relevant polystyrene polymers is essential. Determining optimum conditions for biofilm formation using one variable at a time (OVAT) is laborious and inaccurate. Therefore, mathematical modelling for design of experiments to optimize conditions for biofilm formation in *Candida* species was undertaken. In this study, a simple and robust statistical method, response surface methodology (RSM) was used to optimize independent variables like temperature, incubation period, media pH, shaker speed and inoculum density. Biofilm forming conditions were optimized and compared for two important local clinical isolates and one standard culture on 96 well polystyrene microtiter plates. Biofilm was quantified by different methods, like XTT for cell viability, crystal violet for biofilm, calcofluor white, and wet and dry weight measurements for cell mass. Quantification of cell viability and biofilm indicated heterogeneity among the three cultures. The results revealed an important finding that foetal bovine serum (FBS) does not significantly affect biofilm formation *in vitro*. This simple high throughput method for optimization and quantification of *Candida* biofilm has relevance for applications in rapid screening of anti-*Candida* biologics and therapeutic solutions while advancing control measures in polystyrene carriers in hospital settings.

Keywords: *Candida glabrata*, Biofilm, Response Surface Methodology, XTT Assay, Crystal Violet Assay, Calcofluor White Assay

INTRODUCTION

Candida infections from *C. albicans* and *C. glabrata* remain the first and second most frequent cause of fungal infections globally in most of the immunocompromised individuals [1,2]. Several *Candida* species cause candidiasis of the mouth (oral candidiasis), ear (otitic candidiasis), genital tract (Balanitis/Vaginitis), and blood (systemic candidiasis). Invasive candidiasis is a form of nosocomial infection [3]. The most essential and dangerous characteristic of *Candida* species is their ability to form biofilms [4], which contribute to challenges for therapeutic solutions and disease control. Biofilm is a community of sessile microorganisms/cells that grow by attaching to a surface or each other and is embedded in an exopolysaccharide matrix [5,6]. Extracellular polysaccharide, a conditioning film acts as a bridge between the organisms [7]. Biofilm has a high level of organization forming a 3D structure [8]. The microbes in biofilm exhibit a coordinated behavior and live in cooperative consortia [9]. The pathogenicity of *Candida* species is mainly attributed to certain factors such as adhesion to polymeric medical devices and/or host cells, biofilm formation, and secretion of hydrolytic enzymes [3]. Biofilm acts as a protective shield and its structure causes slow diffusion of therapeutic antifungals within its interior, thus interfering with disease control [10,11].

Candida glabrata with its virulence factors is highly resistant to antifungal drugs and its ability to form biofilm leads to systemic infections. The importance of biofilms is underlined by their characteristic feature of exhibiting resistance to host defensive mechanisms, antimicrobial treatment resistance, and biofouling of medical devices [12,13]. The pathogenic behavior starts immediately with colonization and penetration of the intestinal mucosa and movement to the bloodstream [14]. The most isolated fungal species from the large array of infections include *C. albicans*, *C. glabrata*, *Candida parapsilosis*, *Candida tropicalis*, and *Candida guilliermondii* [15]. Most mycological studies have revealed *Candida* infections due to non-*Candida albicans* Candida (NCAC), mainly *C. glabrata* [16]. About 29% of bloodstream infections are due to *C. glabrata* [17]. *C. glabrata* lacks the ability to form hyphae and secrete proteases and hence the mechanism of its tissue invasion remains largely unexplored. However, it associates with biotic/abiotic polymeric surfaces to form a biofilm [18,19] where therapeutics can be targeted. This necessitates the essential need to overcome *C. glabrata* associated biofilm infections and to understand the underlying mechanism for its resistance to antifungal drugs [20] and improve screening and targeting of therapeutics.

Recent studies on *C. glabrata* have focused on the phenotypic switching that leads to biofilm formation [21,22]. Biofilm formation

†To whom correspondence should be addressed.
E-mail: bindu@msrit.edu, bindu.sadanandan@gmail.com

is a complex process governed by several factors, such as the choice of material, the type, composition, and pH of media [23]. *In vitro* biofilm formation studies have reported the use of FBS for adhesion of *Candida* cells to polymeric substrata [24]. Surface adhesion of cells to the abiotic polymeric substratum is the first step towards colonization and biofilm formation. The surface precoating of the wells or use of media supplemented with FBS has been reported to enhance firm attachment of cells, which eventually influences biofilm formation [25,26]. Therefore, it is imperative to develop robust methods to study independent factors that contribute towards biofilm formation in hospital relevant polymeric substratum. Response surface methodology (RSM) is the preferred approach to overcome systematic and random errors during media optimization studies. Among several available RSM based experimental design tools, central composite design (CCD) is most routinely used for the optimization of culture conditions. As a high-resolution design, CCD imparts essential quality to experimental design matrix, such as uniformity, rotatability and orthogonality, thus accounting for one of the most robust designs. The CCD model can be tested and validated by using second-order polynomial regression equation along with surface plots [27,28]. We have optimized growth conditions for biofilm formation of *C. glabrata* on polystyrene polymeric material. This study advances the effective optimization of growth conditions for biofilm formation in *Candida* species using mathematical modelling and design of experiments. The conditions for biofilm formation, quantification, and relationship to cell viability and cell mass will provide vital clues into understanding the virulence of *C. glabrata* and designing appropriate biofilm control measures. This also provides a relevant screening tool for screening new anti-Candida therapeutics.

Therefore, the present study performed a comparative assessment of biofilm formation by standard culture MTCC 3019 and clinical isolates M-2196 and D-5 from local hospital infections. The independent variables that are conducive for biofilm formation were optimized *in vitro* using RSM on polystyrene material (discs and plates) relevant in hospitals. The effect of physicochemical factors--pH of media, temperature, incubation period, shaker speed, and inoculum density on biofilm formation for the three selected cultures of *C. glabrata*--were standardized by CCD design. Biofilm formed by *C. glabrata* cultures was quantified using different assays such as XTT, crystal violet, calcofluor white dye binding, wet and dry weight measurements, as each method was measured and revealed different aspects of the biofilm formation.

MATERIALS AND METHODS

1. Organisms

A total of three *C. glabrata* cultures, a standard MTCC 3019 and two local hospital clinical isolates M-2196 and D-5 from catheter vein tip and dental sample, respectively, of female patients with invasive candidiasis, were used in this study. The local hospital clinical isolates were obtained from the Microbiology Laboratory at M S Ramaiah Medical College and Teaching Hospital, Bengaluru, India. *C. glabrata* MTCC 3019 (ATCC 90030) was procured from IMTECH, Chandigarh, India. Ethical Clearance for the use of clinical isolates of *C. glabrata* was not mandatory, as no human subjects were directly involved in the study. Clinical isolates were identified using Lactophenol cotton blue test [29], germ tube test [30] and colony morphology on CHROMagar *Candida* (CHROMagar, growth at 45 °C) [31].

2. Substrate Material

Sterile 5 mm polystyrene discs and 96 well polystyrene microtiter plates were used as polymeric substratum due to their similarity with the materials used in medical prosthetics and because of the ease in handling.

3. Medium and Culture Conditions

Standard culture, as well as clinical isolates, were subcultured every 15 days on Malt Yeast Agar (MYA) slopes/agar plates and incubated at 37 °C for immediate use. Glycerol stocks were also maintained and stored at −20 °C. Fresh cultures were prepared in RPMI-1640 (HiMedia AL028A-100ML) and incubated for 24 h at 30 °C in an incubator shaker at 60 rpm for growth optimization studies and biofilm formation.

4. Growth OD and Cell Enumeration

Growth measurements of *C. glabrata* were carried out in RPMI-1640 medium using a UV visible spectrophotometer at 600 nm. Haemocytometry was performed to adjust the initial cell density to 10^6 cells ml^{-1} and used as stock. The experiment was performed in triplicate.

Experiments were performed with and without FBS precoating in the wells of the microtiter plates in order to check its effect on cell adherence, which in turn induces biofilm formation.

5. Biofilm Formation on Polystyrene Material and Optimization using RSM

C. glabrata biofilm was induced in 96 well microtiter plates with modifications to the protocol from a published study [24]. In this study, a step involving the precoating of wells with FBS was excluded as there was no significant difference in the output in the experiments carried out with and without FBS. Hence further experiments were carried out without precoating with FBS. The stock suspension of 10^6 cells ml^{-1} was used to prepare different inoculum densities of 10^4, 4×10^4, 7×10^4, 10^5 and 1.3×10^5 cells ml^{-1}. A volume of 100 µl of each inoculum density was added to the wells of flat bottom 96-well microtiter plate with discs to ensure uniform growth in an incubator for 90 min at 37 °C for adhesion. After incubation, the medium was discarded, and wells of microtiter plates were washed twice with 1X phosphate-buffered saline (PBS) to discard non-adherent cells. Following this, 100 µl of fresh RPMI-1640 with pH adjusted to 5.5, 6.5, 7.5 and 8.5 was added to the wells containing the discs. The plates were sealed with parafilm to prevent evaporation and incubated at temperatures of 25, 30, 35, 40 and 45 °C at growth periods of 7, 25, 42, 60 and 77 h in an incubator shaker at speeds of 20, 40, 60 and 80 rpm. The results obtained were quantified with XTT by measuring OD at 492 nm.

6. Response Surface Optimization of Biofilm Formation by Clinical Isolates

The above-mentioned culture conditions for *C. glabrata* cultures were optimized by RSM to study the interactions and responses between the independent variables [32]. High resolution full factorial CCD was used to optimize the culture conditions to facilitate the standardization of interactions of factors without any systematic and random error. The culture condition range for each inde-

Table 1. Design Matrix and XTT response for *C. glabrata* cultures

Sl. No	Temp °C	pH	Incubation period (h)	Inoculum size (cells ml^{-1})	Shaker speed (rpm)	MTCC 3019		M 2196		D5	
						Obs	Pred	Obs	Pred	Obs	Pred
1	30	5.5	25	4	60	1.29	1.22	1.37	1.35	1.32	1.31
2	30	5.5	25	10	20	0.80	0.82	0.71	0.71	0.66	0.67
3	30	5.5	60	4	20	0.56	0.58	0.56	0.57	0.53	0.53
4	30	5.5	60	10	60	0.22	0.16	0.24	0.24	0.23	0.23
5	30	7.5	25	4	20	0.90	0.91	0.80	0.80	0.75	0.75
6	30	7.5	25	10	60	1.14	1.08	1.18	1.17	1.32	1.32
7	30	7.5	60	4	60	0.06	0.01	0.13	0.12	0.07	0.06
8	30	7.5	60	10	20	0.62	0.65	0.66	0.67	0.65	0.66
9	40	5.5	25	4	20	0.40	0.41	0.61	0.61	0.62	0.62
10	40	5.5	25	10	60	0.92	0.85	0.90	0.89	0.98	0.98
11	40	5.5	60	4	60	0.70	0.65	0.64	0.64	0.70	0.69
12	40	5.5	60	10	20	0.56	0.58	0.53	0.54	0.52	0.52
13	40	7.5	25	4	60	0.97	0.91	0.89	0.88	1.00	0.99
14	40	7.5	25	10	20	0.42	0.43	0.41	0.42	0.38	0.39
15	40	7.5	60	4	20	0.56	0.58	0.53	0.54	0.49	0.49
16	40	7.5	60	10	60	0.68	0.62	0.72	0.72	0.66	0.66
17	25	6.5	42	7	40	0.55	0.59	0.67	0.67	0.61	0.60
18	45	6.5	42	7	40	0.43	0.48	0.55	0.55	0.54	0.54
19	35	4.5	42	7	40	0.44	0.49	0.49	0.49	0.46	0.46
20	35	8.5	42	7	40	0.43	0.47	0.43	0.43	0.40	0.40
21	35	6.5	7	7	40	1.13	1.19	1.12	1.14	1.34	1.34
22	35	6.5	77	7	40	0.44	0.46	0.43	0.41	0.52	0.51
23	35	6.5	42	1	40	0.44	0.49	0.51	0.52	0.50	0.51
24	35	6.5	42	13	40	0.43	0.47	0.48	0.48	0.51	0.50
25	35	6.5	42	7	0	0.62	0.50	0.49	0.47	0.35	0.33
26	35	6.5	42	7	80	0.45	0.65	0.75	0.78	0.73	0.75
27	35	6.5	42	7	40	0.33	0.25	0.22	0.22	0.23	0.23

Observed, Obs; Predicted, Pred

pendent factor was defined based on standardized studies. The experimental test range for the selected independent factor(s), 27 experimental runs, observed and predicted XTT values are shown in Table 1.

The second-order polynomial regression equation was used to assess correlation between the observed and predicted values of dependent variables, which was calculated by using Eq. (1):

$$Y = \beta_o + \Sigma_{i=1}^{n}\beta_i X_i + \Sigma_{i=1}^{n}\beta_{ii} X_i^2 + \Sigma_{\substack{i-1\\ j>i}}^{n-1}\Sigma_{j=2}^{n}\beta_{ij} X_i X_j \quad (1)$$

where, Y is a dependent variable (obtained XTT value), β_0 is constant coefficient; β_i, β_{ii}, β_{ij} are coefficient of linear, quadratic and their interactions of independent factors, respectively. X_i and X_j are input independent variables that influence the response of dependent variable Y. The design was analyzed by STATISTICA (version 12.6) statistical software; analysis was based on analysis of variance (ANOVA) where the design was analyzed based on the p value. Further, the standardized effect of independent variables was calculated and represented in the form of a Pareto chart. The standardized effect (E_{xi}) of independent variables was calculated using Eq. (2):

$$E_{xi} = \frac{2(\Sigma P_{i+} - \Sigma P_{i-})}{N} \quad (2)$$

where, P_{i+} and P_{i-} represent response of independent factor at higher and low experimental levels, respectively.

7. Biofilm Quantification Methods

Biofilm formed by *C. glabrata* cultures on polystyrene material was quantified using the following methods: XTT [2,3-bis-(2-methoxy-4-nitro-5-sulfophenyl)-5-[(phenylamino)carbonyl]-2H-tetrazolium hydroxide] reduction assay; crystal violet dye binding assay and calcofluor white dye binding assay along with wet weight and dry weight measurements. All assays were performed in quadruplicate. Statistical analysis was performed for the selected bioassays using one way ANOVA by adopting Sidak's multicomparison test.

8. XTT Assay

XTT reduction assay was carried out as described previously by [33]. Biofilm growth was induced directly in the wells of polystyrene microtiter plates. XTT[2,3-bis-(2-methoxy-4-nitro-5-sulfophenyl)-5-[(phenylamino)carbonyl]-2H tetrazolium hydroxide] was prepared in 1 ml PBS (1 mg ml^{-1}) and Phenazine methosulfate (PMS)

was prepared in 1 ml H_2O (0.32 mg ml^{-1}). Following the biofilm formation phase, medium was discarded, and the wells were washed twice with PBS. To each well, 90 µl of XTT and 10 µl PMS were added. The plates were incubated in dark at 37 °C for 30 min. The absorbance for each well was recorded using an automated multimode microplate reader (Synergy HT, BIOTEK) at 492 nm.

9. Crystal Violet (CV) Assay

Biofilm formation and quantification by crystal violet assay was followed as described by [34]. Excess medium was removed and the wells containing biofilm were washed twice with PBS. A volume of 100 µl of 1% crystal violet (1% in water) was added to each well and incubated for 20 min at 37 °C. The dyed biofilm was dissolved in 150 µl of 95% ethanol. Following this, 100 µl of each of these mixtures was transferred to new 96 well plates and absorbance was recorded using an automated multimode microplate reader at 570 nm.

10. Calcofluor White Assay (CWA)

Biofilm was induced in 96 well microtiter plates. Calcofluor White M2R from 5 mM stock solution was prepared to a final concentration of 25 µM and added to staining solution (Buffer A: 2% D Glucose, 10 mM Na-HEPES, pH 7.2). After biofilm formation 100 µl staining solution was added to each well and incubated in dark at 30 °C for 45 min. Staining solution was removed and 100 µl TE buffer [Buffer B: 10 mM Tris HCl, pH 8.0, 10 mM EDTA] was added. Fluorescence was measured at an excitation wavelength of 360 nm and emission wavelength of 460 nm using an automated multimode microplate reader [35].

11. Wet Weight and Dry Weight Measurements

Wet weight measurements were performed by inducing biofilm growth on polystyrene discs placed within 96 well microtiter plate. After biofilm formation, the discs were carefully lifted from the well and washed with PBS to remove the non-adherent cells. The discs were then weighed, which represented the entire hydrated mass of biofilm [24].

Dry weight measurements were carried following a previously published method [36]. Biofilm growth was induced on polystyrene discs in 96 well microtitre plate. After biofilm formation, the medium was drained. Biofilm on the discs was scraped and dissolved in PBS and then filtered through preweighed filter disc with a pore size of 0.45 µm. The discs were dried in hot air oven at 35 °C for 24 h and weighed. The weight of biofilm was calculated by subtracting the weight of filter dics before and after filtration.

RESULTS

1. Optimization of Physical Conditions for Growth of *C. glabrata* Biofilm using RSM

C. glabrata species rapidly adapt to diverse environmental conditions of pH, temperature, incubation time and hospital relevant non-biological polymeric surfaces to form a biofilm. Thus, in the present investigation, different physical parameters along with varying inoculum density from 10^4-10^5 cells ml^{-1} (biological parameter) were chosen to optimize biofilm formation for selected local clinical isolates of *C. glabrata* M-2196 and D-5 using RSM. The culture conditions were compared and validated against biofilm forming standard culture *C. glabrata* MTCC 3019 based on XTT value. The statistical analysis and comparison were based on a high-resolution CCD design, which was further analyzed by Pareto chart, ANOVA, and second-order polynomial regression equation. The CCD model predicted solution at the critical level was further experimentally validated. The Pareto chart indicated that incubation period and shaker speed, in general, have a more significant role (p=0.05) on biofilm formation for MTCC-3019, M-2196, and D-5 (Fig. S1).

The ANOVA is the most used statistical analysis for the identification of significant factor(s) that affect study results. The sum of squares (SS) indicates the deviation among the data set(s) from the mean value. SS also possess the variability existing among the datasets; a lower quantitative value indicates no significant deviation from the mean value. The degree of freedom (DF) expresses the number of independent factor(s) that are considered for the calculation. F value is the ratio of mean square effect and it also plays an important role in the rejection of the null hypothesis when the value is greater than 1. The p value indicates the probability of the observed results to substantiate the null hypothesis, where the lowest p value provides a strong lead to reject the null hypothesis. ANOVA is used to identify the significant independent factor(s) considered in the study. Critically, from the analysis point of view, the F and the p values derived from ANOVA are considered. In the present investigation for the selected strains of *C. glabrata* temperature, shaker speed and incubation period significantly affected the XTT value. For *C. glabrata* MTCC 3019 the temperature and incubation period, i.e., 1 L by 3 L has exhibited the significant interaction (F value of 21.03908 and p value 0.003743). In case of M-2196 and D-5 local strains, incubation period and shaker speed were found to be significant, i.e., 3 L by 5 L which exhibited F value of 710.528 and 1651.857 and p value of <0.001, respectively (Table 2).

The second-order polynomial regression equation provides insight into the interaction among physicochemical factors and their effect on the response, i.e., XTT value for the selected cultures of *C. glabrata,* which was calculated by using Eqs. (3), (4), and (5) respectively. The equations indicate the influence of independent factors (linear and quadratic forms) and their interactions on XTT value.

$$Y_{MTCC3019}=12.33-0.33073x_1+0.00283x_1^2-0.87386x_2+0.05696x_2^2 -0.09496x_3+0.00047x_3^2+0.00176x_1x_3+0.00094x_1x_5-0.00043x_3x_5 \quad (3)$$

$$Y_{M2196}=13.72-0.36031x_1+0.0390x_1^2-1.02189x_2+0.005989x_2^2 -0.09870x_3+0.00045x_3^2-0.3431x_4+0.00763x_4^2-0.01469x_5 +0.00025x_5^2+0.03x_1x_3+0.00055x_1x_5+0.00136x_2x_3+0.02958x_1x_4 -0.00090x_3x_4-0.00042x_3x_5 \quad (4)$$

$$Y_{D5}=10.98224-0.28521x_1+0.0390x_1^2-0.71222x_2+0.04939x_2^2 -0.09476x_3+0.00057x_3^2+0.28301x_4+0.00757x_4^2-0.01064x_5 +0.00019x_5^2-0.00425x_1x_2+0.00140x_1x_3-0.00192x_1\ x_4+0.0061x_1x_5 +0.03083x_2x_4+0.000743x_2x_4-0.00049x_3x_5+0.00029\ x_4x_5 \quad (5)$$

where, Y=XTT value for the biofilm formed, =Incubation temperature, =pH, =Incubation period, =Inoculum size, =Shaker speed.

The curvilinear 3D response surface plots indicating XTT value on Z-axis against the variables that profoundly affected biofilm formation for *C. glabrata* MTCC 3019 and clinical isolates M-2196 &

Table 2. Analysis of variance of physicochemical factors on biofilm formation

Cultures	Factor	SS	df	MS	F	p
MTCC 3019	(1) Temperature (°C) (L)	0.014250	1	0.014250	0.79229	0.407680
	Temperature (°C) (Q)	0.080017	1	0.080017	4.44875	0.079460
	(2) pH (L)	0.000620	1	0.000620	0.03448	0.858809
	pH (Q)	0.051924	1	0.051924	2.88687	0.140218
	(3) Incubation period (h) (L)	0.729567	1	0.729567	40.56241	0.000704
	Incubation period (h) (Q)	0.333492	1	0.333492	18.54148	0.005060
	(4) Inoculum size (cells·ml^{-1}) (L)	0.000361	1	0.000361	0.02010	0.891904
	Inoculum size (cells·ml^{-1}) (Q)	0.051924	1	0.051924	2.88687	0.140218
	(5) Shaker speed (rpm) (L)	0.025699	1	0.025699	1.42880	0.277057
	Shaker speed (rpm) (Q)	0.107502	1	0.107502	5.97687	0.050146
	1 L by 3 L	0.378415	1	0.378415	21.03908	0.003743
	1 L by 5 L	0.140625	1	0.140625	7.81845	0.031322
	3 L by 5 L	0.366675	1	0.366675	20.38634	0.004038
M-2196	(1) Temperature (°C) (L)	0.016550	1	0.016550	33.851	0.001133
	Temperature (°C) (Q)	0.151786	1	0.151786	310.455	0.000002
	(2) pH (L)	0.005238	1	0.005238	10.713	0.016969
	pH (Q)	0.057403	1	0.057403	117.408	0.000037
	(3) Incubation period (h) (L)	0.726800	1	0.726800	1,486.557	0.000000
	Incubation period (h) (Q)	0.307214	1	0.307214	628.359	0.000000
	(4) Inoculum size (cells·ml^{-1}) (L)	0.002188	1	0.002188	4.475	0.078792
	Inoculum size (cells·ml^{-1}) (Q)	0.075400	1	0.075400	154.219	0.000017
	(5) Shaker speed (rpm) (L)	0.127051	1	0.127051	259.864	0.000004
	Shaker speed (rpm) (Q)	0.159679	1	0.159679	326.598	0.000002
	1 L by 3 L	0.270475	1	0.270475	553.215	0.000000
	1 L by 5 L	0.048400	1	0.048400	98.995	0.000060
	2 L by 3 L	0.009023	1	0.009023	18.454	0.005116
	2 L by 4 L	0.126025	1	0.126025	257.765	0.000004
	2 L by 5 L	0.003025	1	0.003025	6.187	0.047328
	2 L by 4 L	0.126025	1	0.126025	257.765	0.000004
	3 L by 5 L	0.347388	1	0.347388	710.528	0.000000
D-5	(1) Temperature (°C) (L)	0.003552	1	0.003552	12.522	0.012239
	Temperature (°C) (Q)	0.117370	1	0.117370	413.763	0.000001
	(2) pH (L)	0.005391	1	0.005391	19.004	0.004774
	pH (Q)	0.039040	1	0.039040	137.626	0.000023
	(3) Incubation period (h) (L)	0.936274	1	0.936274	3,300.620	0.000000
	Incubation period (h) (Q)	0.486823	1	0.486823	1,716.183	0.000000
	(4) Inoculum size (cells·ml^{-1}) (L)	0.000109	1	0.000109	0.384	0.558042
	Inoculum size (cells·ml^{-1}) (Q)	0.074305	1	0.074305	261.945	0.000004
	(5) Shaker speed (rpm) (L)	0.240145	1	0.240145	846.577	0.000000
	Shaker speed (rpm) (Q)	0.094613	1	0.094613	333.535	0.000002
	1 L by 2 L	0.007225	1	0.007225	25.470	0.002341
	1 L by 3 L	0.240268	1	0.240268	847.010	0.000000
	1 L by 4 L	0.013225	1	0.013225	46.622	0.000485
	1 L by 5 L	0.060025	1	0.060025	211.604	0.000007
	2 L by 4 L	0.136900	1	0.136900	482.610	0.000001
	3 L by 4 L	0.023930	1	0.023930	84.360	0.000094
	3 L by 5 L	0.468576	1	0.468576	1,651.857	0.000000
	4 L by 5 L	0.004900	1	0.004900	17.274	0.005970

Linear, L; Quadratic, Q; sum of the square, SS; degree of freedom, df; Mean square MS

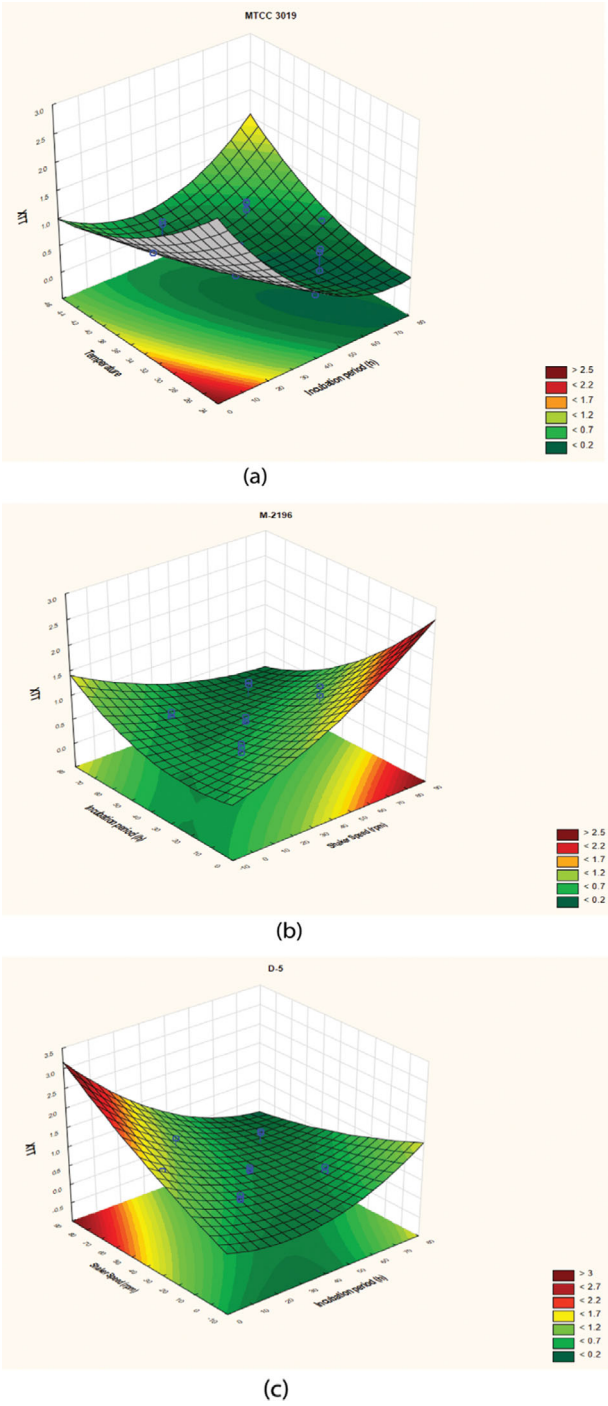

Fig. 1. 3D Response surface plots for *C. glabrata* cultures depicting the interaction of independent variables for the selected *C. glabrata* cultures (a) MTCC 3019 (Incubation period vs Temperature (b) M-2196 (Incubation period vs Shaker speed) (c) D-5 (Incubation period vs Shaker speed). The marked labels indicate the fractional factorial design with center points, augmented with a group of axial points, i.e., $-\alpha$, -1, 0, $+1$, $+\alpha$ for *C. glabrata* cultures. The blue dots mark the intersection point for x, y & z coordinates (The x, y - independent variable and z - dependent response). The color grade depicts yield gradients for Z coordinate, i.e., XTT value. Dark green and dark brown colors represent minimum and maximum XTT values, respectively.

D-5 are shown in Fig. 1(a), 1(b), and 1(c).

The interaction of temperature and incubation period significantly affected the XTT value for MTCC 3019 at 37.7 °C, pH of 6.3, incubation period of 42.5 h, inoculum density of 7.3%, and shaker speed at 29 rpm with a predicted value of 0.22 and observed experimental XTT response value of 0.199±0.017. The XTT value was profoundly affected by the interaction of the incubation period and shaker speed in case of clinical isolates M-2196 and D5. Whereas for the clinical isolate M-2196, XTT value of 0.25 was predicted at the optimum physicochemical condition of temperature at 45.4 °C, pH of 5.5, incubation period of 9.9 h, inoculum density of 11.7%, and shaker speed at 19.5 rpm, the observed XTT value was 0.225±0.015. The predicted XTT value for D-5 was 0.18 at the optimum conditions of the temperature of 36.8 °C, pH of 6.5, incubation period of 42.9 h, inoculum density of 7.6%, and shaker speed at 24 rpm, whereas the observed experimental XTT value was 0.186±0.001. The model was validated by performing experiments at critical conditions in quadruplicate to observe the closeness of the predicted and observed values (Fig. S2). The optimization of culture conditions by CCD design in our study provided optimal culture conditions for clinical isolates M-2196 and D-5 and for the standard culture *C. glabrata* MTCC 3019 where, interestingly, the lower shaker speed favors biofilm formation for all the selected cultures. The cell adhesion and biofilm formation in RPMI media with and without FBS precoating of polystyrene wells did not show a significant difference (Fig. 2). Hence, biofilm

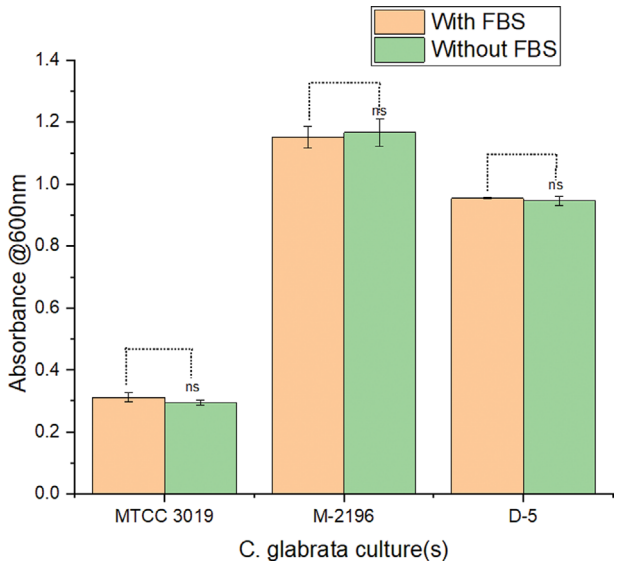

Fig. 2. Cell adhesion in presence and absence of FBS for *C. glabrata* cultures. Cell adhesion studies with and without FBS coating exhibited no significant changes (ns: No significance) analyzed by one-way-ANOVA (Sidak's multi-comparison test for quadruplicate for each tested independent variable). The comparison of cell adhesion of *C. glabrata* cultures MTCC 3019, M-2196 & D-5 was performed on RPMI media in 96 well microtiter plates with and without FBS coating. Absorbance was measured at 600 nm after 24 h. The experiment was performed in quadruplicate. All values are expressed as mean and standard deviation (SD). The error bars represent standard error of the mean.

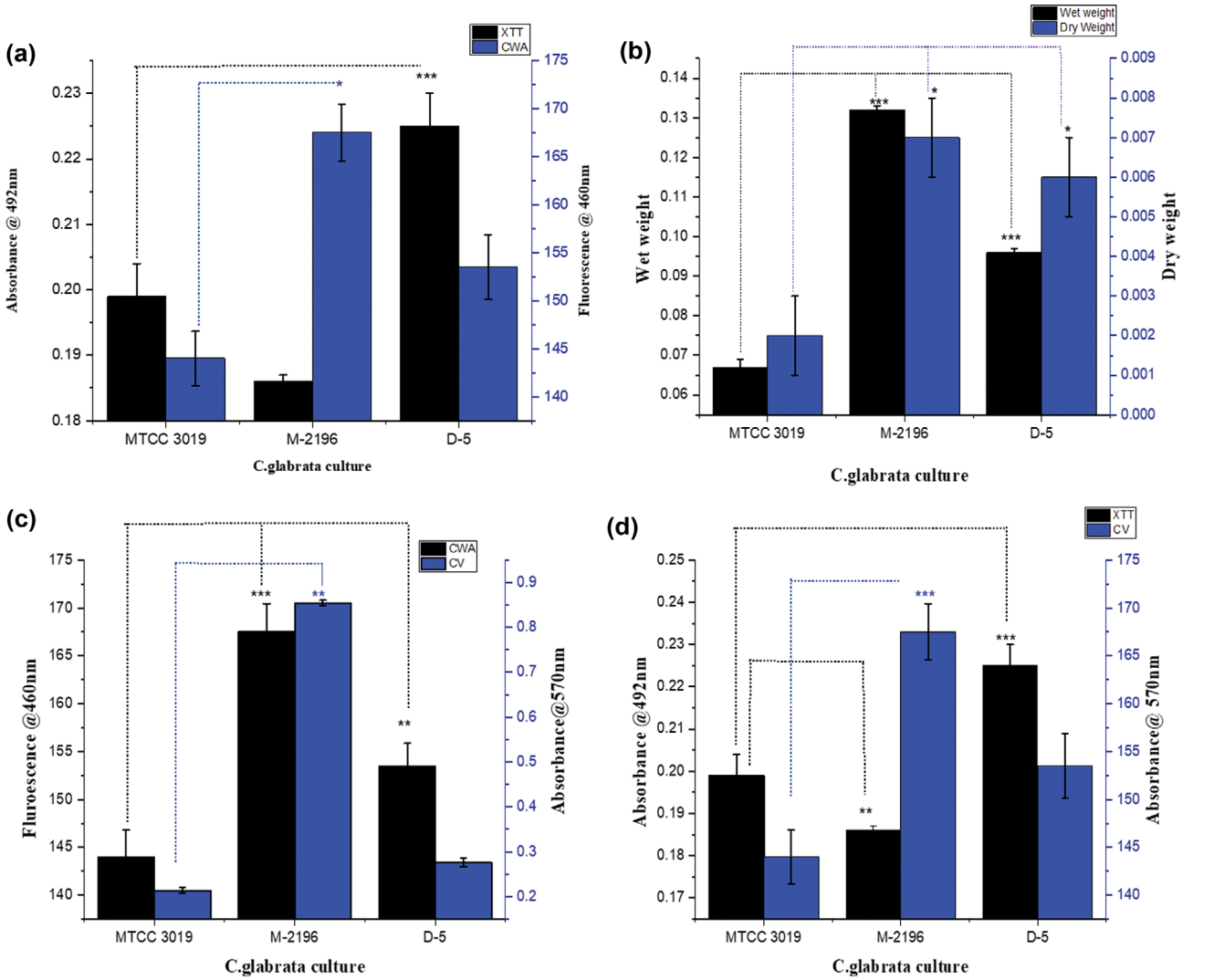

Fig. 3. Correlation of Calcofluor White, XTT, Crystal violet Assays for *C. glabrata* cultures MTCC 3019, M-2196 and D-5. The above graphs represent the correlation of variables for (a) CWA vs XTT, (b) Wet weight vs Dry weight (c) CWA vs CV, (d) XTT vs CV. Assays were performed in quadruplicate. All values are the mean and standard deviation (SD). The error bars represent standard error (SE) of the mean. The statistical significance was obtained by One way ANOVA (Sidak multicomparison test), where one * refers to p<=0.05, ** refers to p<0.01, * refers to p<=0.001.**

studies were carried out further without precoating of wells with FBS.

Cell adhesion studies with and without FBS coating exhibited no significant changes (ns: No significance) analyzed by one-way-ANOVA (Sidak's multi-comparison test for quadruplicate for each tested independent variable). The comparison of cell adhesion of *C. glabrata* cultures MTCC 3019, M-2196 and D-5 was performed in RPMI media in 96 well microtiter plates with and without FBS coating. Absorbance was measured at 600 nm after 24 h. The experiment was performed in quadruplicate. All values are expressed as mean and standard deviation (SD). The error bars represent standard error (SE) of the mean.

2. Quantification of *C. glabrata* Biofilm

In the present investigation the statistical significance of the response assays--XTT, Calcofluor White (CWA) and Crystal Violet (CV) along with wet and dry weight measurements for *C. glabrata* cultures--were analyzed by one way ANOVA using multi-comparison Sidak test. In case of XTT vs CWA assay, the clinical isolate D5 possesses significant XTT value (p value of <0.001) as compared to clinical isolate M2196, which was found to be insignificant, whereas in case of CWA assay M2196 clinical isolate was found to be significant (p<0.05), as shown in Fig. 3(a). Significant variations were observed in the wet weight (p value of <0.001) and dry weight measurements (p value of <0.05) of the cultures tested, as shown in Fig. 3(b). Interestingly, for the strain D5, CV assay was not found to be significant as compared to other assays, i.e., CWA and XTT as shown in Fig. 3(c) and 3(d), respectively.

Quantified cell viability in ascending order for tested *C. glabrata* cultures based on XTT assay:

MTCC 3019>D-5>M-2196.

Quantified cell mass in ascending order for tested *C. glabrata* cultures based on calcofluor white assay and wet and dry weight mea-

surements:

D-5>MTCC 3019>M-2196.

Quantified biofilm in ascending order for tested *C. glabrata* cultures based on crystal violet assay:

M-2196>D-5>MTCC 3019.

DISCUSSION

Candidemia research has shifted from *C. albicans* and moved more towards the NCAC member, *C. glabrata* [37], as it is most prevalent in severe cases of systemic candidemia [38]. Candidemia triggers life-threatening complications in immunocompromised individuals [39]. *Candida* pathogenesis is mainly attributed to its ability to form biofilm communities, which extends to hospital polymeric materials.

The study is very significant, as *C. glabrata* is the second most biofilm-forming species among genus *Candida* [2]. Biofilm formation depends on both initial cell density [40] and physiological conditions. Growth OD measurements at 600 nm followed by haemocytometry to adjust the initial cell density are crucial to obtain consistency and optimize conditions for biofilm formation. There are few studies on *Candida* species indicating the correlation between cell density, their adhesion to clinically relevant non biological polymeric surfaces, and biofilm formation [3,41]. Adhesion to biotic surfaces like mucous membranes and abiotic surfaces like acrylic [10] and polystyrene is a major prerequisite for biofilm formation; therefore, initial cell densities play a significant role in biofilm formation. In *C. glabrata,* biofilm formation is also closely associated with alterations in gene expression and mutation, which eventually also leads to the development of antifungal resistance [42].

The present investigation demonstrates the usefulness of statistical design of experiments such as RSM in optimizing conditions for biofilm forming clinical isolates. The conventional method of optimizing conditions for biofilm formation using one-variable-at-a-time (OVAT) is laborious and referred as to statistically insignificant as it leads to systematic and randomized errors. In statistical research CCD is regarded as a statistical design of experiment (DoE) used to perform RSM studies to investigate the interaction and optimization of processing or culture conditions. CCD is typically a two-block orthogonal study between star or axial and center points and factorial portion. The CCD model typically predicts optimized high yielding point (obtained by second-order polynomial regression equation), which must be cross validated experimentally. CCD design is a full fractional factorial design regarded as one of the high-resolution study designs, as each independent factor is tested at five levels ($-\alpha, -1, 0, +1, +\alpha$) where $-\alpha$ and $+\alpha$ refer to axial points of the design, unlike other factorial design such as box Behnken or Plackett Burman. In the study, CCD design not only separates the random noise or screens the independent physicochemical factors that are affecting biofilm formation, but also provides significant interaction study details among tested variable(s) and determines the critical optimized parameters for culturing and for further investigation [43,44].

RSM is a superior and simpler approach for optimization studies as it consists of a collection of statistical tools to design, analyze and validate the experimental conditions [45]. The statistical use of CCD in RSM helps to achieve an effective relationship between independent variables and obtained responses as the design has better resolution. In the present investigation, different physicochemical factors were optimized for biofilm forming local clinical isolates M-2196 and D-5, compared and validated against biofilm forming standard culture MTCC 3019. The study also helped to identify critical physicochemical factors influencing biofilm formation in a polystyrene matrix.

As per published literature, the coating of surfaces with foetal bovine serum (FBS) or the use of FBS supplemented media is mandatory for the adhesion of biofilm [26,46]. However, peeling off of biofilm formed on FBS precoated surfaces has also been reported [25]. The present investigation has revealed that FBS precoating does not significantly influence cell adhesion to substratum and thereby biofilm formation in *C. glabrata*.

Non-invasive *Candida* species show higher levels of XTT activity as compared to invasive species [47].

Some of the widely used semiquantitative methods to study cell viability, biofilm and biomass are XTT assay, crystal violet assay, calcofluor white assay, wet and dry weight measurements. Each assay addresses a specific characteristic of the pathogen. Quantifying biofilms using semi quantitative XTT - cell viability assay in multiwell plates and discs is widely used [5,21,48,50,59]. However, as the viability of cells does not accurately determine biofilm formation, the use of both approaches, i.e., XTT and CV assays, would help in understanding of viability as well as biofilm forming potential that determine the clinical behavior of the isolate [6]. Crystal violet assay, calcofluor white assay, wet and dry weight methods are also used for quantifying the biofilm, as the use of XTT assay is only based on the metabolic activity of cells [51], which may vary in planktonic and biofilm phase cells [26]. XTT reduction assay is often being used to estimate the impact of anti-biofilm strategies, as it gives a measure of a viable cell count [52]. However, the approach of employing four different biochemical quantification methods in this study not only provided the advantage of comparing the cell viability, biofilm formation and cell mass in *C. glabrata*, but also helped in better understanding of biofilm characteristics, as each method revealed different aspects of the biofilm. This simple foF-Fur-pronged approach for optimization and quantification of biofilm has been adopted as it provides an effective model for comprehensive biofilm studies and for further screening of critical anti-Candida therapeutic solutions.

Quantification of cell viability and biofilm indicated heterogeneity among the three cultures. Strain-wise difference is seen due to the niches in that they have been dwelling. Strong and selective control of microbes inhabiting different human body sites like oral mucosa, skin, gut and urinogenital tract is observed for colonization and survival in their habitats [53]. The hallmarks of virulence, such as cell viability, biofilm formation and cell mass, may vary in different strains due to their wide diversity and clinical origin. From an evolutionary point of view, it suggests that the hyphal transition of *Candida* cell is the most crucial factor for pathogenicity and invasion into host tissues, which in turn is dependent on its ability to adapt to different niches [53,54]. Based on the ecological niche

that these strains have adapted to in the human host, their characteristics and manifestations of virulence and biofilm formation change accordingly. The strain-wise difference in pathogenicity has serious ramifications in clinical settings with reference to disease prognosis and treatment regime. The differential responses of the clinical isolates to biofilm therapies are largely dependent on their capacity to form biofilm [55]. Therefore, a 'one treatment plan for all' approach often does not work well even for the same species due to the strain-wise heterogeneity of pathogenic species.

The three *C. glabrata* cultures used in our study were isolated from catheter vein tip (M-2196), dental sample (D-5) and blood (MTCC-3019); therefore, all three of them belong to different strains that have adapted to their habitat and exhibit characteristics suitable for their growth and persistence. The heterogeneity observed in cell viability, biofilm formation and cell mass of *C. glabrata* strains in our study likewise points towards strain-wise diversity prevalent in infectious species and the potential to adapt to non-biological polymeric materials in hospital settings.

CONCLUSIONS

Candida glabrata, owing to its virulence factors, leads to biofilm causing systemic infections that are highly resistant to antifungal drugs. In this study, optimization of growth conditions for biofilm formation of *C. glabrata* on polystyrene material was investigated. The conditions for biofilm formation, quantification, and relationship to cell viability and cell mass will provide vital clues into understanding the virulence and designing appropriate biofilm control measures. Strain-wise distinctness in cell viability, biofilm and cell mass was observed for the cultures tested. The results from this investigation indicate that, for the cultures where the viability of cells was high, biomass was low and vice versa. However, biofilm was found to be independent of these two characteristics. Through this study, a simple high throughput method for optimization and quantification of *Candida* biofilm on polystyrene material relevant in hospital settings was developed. The results of our study reveal an important finding that foetal bovine serum (FBS) does not significantly affect cell adhesion and thereby biofilm formation *in vitro*. The results are significant as there are no previous reports of the optimization of conditions for biofilm formation by *Candida* species using mathematical modelling and design of experiments. This has implications for biofilm formation and pathogenicity behavior in hospital polymeric matrix, such as polystyrene and their transfer of potential infections or their control using therapeutics.

ACKNOWLEDGEMENTS

Financial support by DST, Govt. of India, grant no. SR/FT/LS-124/2012 to Bindu Sadanandan, principal investigator is acknowledged. Dr Beena Hemanth wishes to thank Dr Rameez Raja and Dr Indumati V A from M S Ramaiah Medical College and Teaching Hospital, Bengaluru for their help with the isolation of the cultures.

AUTHOR CONTRIBUTIONS

B.S., designed and carried out the experimental work. P.A., A.P.J. and V.V., also carried out the experimental work. L., K. N., supported with the RSM design of experiments. K.S., was involved in the designing of the experiments, analyzing the results and manuscript review. B.H., provided the clinical isolates. B.S., P. A., and L.K.N., drafted the manuscript. All authors reviewed and approved the manuscript.

FUNDING INFORMATION AND CONFLICT OF INTEREST

Financial support was provided by Department of Science and Technology (DST) Government of India. The authors have no conflict of interest. The funders have no role in the study design, data collection interpretation or the decision to submit the work for publication.

SUPPORTING INFORMATION

Additional information as noted in the text. This information is available via the Internet at http://www.springer.com/chemistry/journal/11814.

REFERENCES

1. C. G. Pierce., P. Uppuluri, S. Tummala and J. L. Lopez-Ribot, *J. Vis. Ex.*, **44**, e2287 (2010).
2. Q. Li, J. Liu, J. Shao, W. Da, G. Shi, T. Wang, D. Wu and C. Wang, *Front. Microbiol.*, **10**, 1600 (2019).
3. A. Silva-Dias, I. M. Miranda, J. Branco, M. Monteiro-Soares, C. Pina-Vaz and A. G. Rodrigues, *Front. Microbiol.*, **6**, 205 (2015).
4. J. E. Nett, R. Zarnowski, J. Cabezas-Olcoz, E. G. Brooks, J. Berhardt, K. Marchillo, D. F. Mosher and D. R. Andes, *Infect. Immun.*, **83**, 4630 (2015).
5. L. Corte, D. Casagrande Pierantoni, C. Tascini, L. Roscini and G. Cardinali, *Microorg.*, **7**, 73 (2019).
6. G. S. Baillie and L. J. Douglas, *Methods Enzymol.*, **310**, 644 (1999).
7. M. A. Pfaller and D. J. Diekema, *Clin. Microbiol. Rev.*, **20**, 133 (2007).
8. M. R. Donlan, *Emerg. Infect. Dis.*, **8**, 881 (2002).
9. P. Li, C. J. Seneviratne, E. Alpi, J. A. Vizcaino and L. Jin, *Antimicrob. Agents. Chemother.*, **59**, 6101 (2015).
10. M. L. De la Cruz-Claure, A. A. Cespedes-Llave, M. T. Ulloa, M. Benito-Lama, E. Dominguez-Alvarez and A. Bastida, *Microorganisms*, **7**, 664 (2019).
11. F. Haque, M. Alfatah, K. Ganesan and M. S. Bhattacharyya, *Sci. Rep.*, **6**, 23575 (2016).
12. C. A. Fux, J. W. Costerton, P. S. Stewart and P. Stoodley, *Trends Microbiol.*, **13**, 34 (2005).
13. J. L. Harding and M. M. Reynolds, *Trends Biotechnol.*, **32**, 140 (2014).
14. T. V. M. Vila and S. Rozental, In: Fungal Pathogenicity, S. Sultan Ed. (2016).
15. R. D. Rossoni, J. O. Barbosa, S. F. Vilela, J. D. dos Santos, P. P. de Barros, M. C. de Azevedo Prata, A. L. Anbinder, B. B. Fuchs, A. O. Jorge, E. Mylonakis and J. C. Junqueira, *PloS One,* **10**, 1 (2015).
16. C. F. Rodrigues and M. Henriques, *Ther. Adv. Infect. Dis.*, **4**, 10 (2017).
17. K. Kumar, F. Askari, M. S. Sahu and R. Kaur, *Microorganisms*, **7**, 39

(2019).
18. M. Galocha, P. Pais, M. Cavalheiro, D. Pereira, R. Viana and M. C. Teixeira, *Int. J. Mol. Sci*., **20**, 2345 (2019).
19. C. F. Rodrigues, S. Silva and M. Henriques, *European J. Clin. Microbiol. Infect. Dis*., **33**, 673 (2013).
20. C. F. Rodrigues, M. E. Rodrigues, S. Silva and M. Henriques, *J. Fungi*., **3**, 11 (2017).
21. C. d'Enfert and G. Janbon, *FEMS Yeast Res*., **16**, 1 (2016).
22. P. Schmidt, J. Walker, L. Selway, D. Stead, Z. Yin, B. Enjalbert, M. Weig and A. J. Brown, *Proteomics*, **8**, 534 (2008).
23. S. Kucharíkova, H. Tournu, K. Lagrou, P. Van Dijck and H. Bujdakova, *J. Med. Microbiol*., **60**, 1261 (2011).
24. J. Chandra, P. K. Mukherjee, S. D. Keidich, F. F. Faddoul, L. L. Hoyer, L. J. Douglas and M. A. Ghannoum, *J. Dent. Res*., **80**, 903 (2001).
25. P. N. Kipanga and W. Luyten, *J. Microbiol. Methods*, **139**, 8 (2017).
26. K. Konecna, I. Nemeckova, A. Diepoltova, M. Vejsova and O. Jandourek, *Curr. Microbiol*., **78**, 2104 (2021).
27. D. C. Montgomery, *Design and analysis of experiments*, John Wiley & Sons Publications, Arizona (2017).
28. J. Yu, Q. Wang, Z. Zhang and X. Li, *The Int. J. Adv. Manuf. Technol*., **88**, 1151 (2017).
29. A. Leck, *Community Eye Health*, **12**, 24 (1999).
30. D. C. Sheppard, M. C. Locas, C. Restieri and M. Laverdiere. *J. Clin. Microbiol*., **46**, 3508 (2008).
31. M. A. Pfaller, A. Houston and S. Coffmann, *J. Clin. Microbiol*., **34**, 58 (1996).
32. A. Ebrahimpour, R. N. Z. R. Abd Rahman, D. H. E. Ch'ng, M. Basri and A. B. Salleh, *BMC Biotechnol*., **8**, 96 (2008).
33. J. Nett, L. Lincoln, K. Marchillo, R. Massey, K. Holoyda, B. Hoff, M. VanHandel and D. Andes, *Antimicrob. Agents. Chemother*., **5**, 510 (2007).
34. X. Li, Z. Yan and J. Xu, *Microbiology (Reading)*, **149**, 353 (2003).
35. M. N. Stagoj, R. Komel and A. Comino, *BioTech*., **36**, 380 (2004).
36. D. M. Kuhn, J. Chandra, P. K. Mukherjee and M. A. Ghannoum, *Infect. Immun*., **70**, 878 (2002).
37. P. Gupta, A. Rastogi, S. Joshi, A. Bhardwaj, K. Misra and N. Kumar, *Indian J. Pharma. Sci*., **80**, 949 (2018).
38. C. F. Rodrigues, A. Correia, M. Vilanova and M. Henriques, *J. Clin. Med*., **8**, 142 (2019).
39. R. Alves, S. L. Kastora, A. Gomes-Gonçalves, N. Azevedo, C. F. Rodrigues, S. Silva, L. Demuyser, P. Van Dijck, M. Casal, A. J. Brown and M. Henriques, *npj Biofilms Microbiomes*, **6**, 1 (2020).
40. C. Rodrigues and M. Henriques, *Genes*, **9**, 205 (2018).
41. M. L. Olson, A. Jayaraman and K. C. Kao, *Appl. Environ. Microbiol*., **84**, e02769-17 (2018).
42. K. W. Nickerson, L. A. Audrey and J. M. Hornby, *Appl. Environ. Microbiol*., **72**, 3805 (2006).
43. B. Kaur, B. Kumar, N. Garg and N. Kaur, *BioMed. Res. Int*., **2015**, Article ID 536745 (2015).
44. D. G. Almeida, R. C. F. Soares da Silva, J. M. Luna, R. D. Rufino, V. A. Santos and L. A. Sarubbo, *Front. Microbiol*., **8**, 157 (2017).
45. R. H. Myers, D. C. Montgomery, G. G. G. Vining, C. M. Borror and S. M. Kowalski, *J. Qual. Tech*., **36**, 53 (2004).
46. M. Leonhard, B. Zatorska, D. Moser and B. Schneider-Stickler, *Biomed Res. Int*., **2019**, Article ID 8051270 (2019).
47. L. Maresova and H. Sychrova, *BioTechn*., **43**, 667 (2007).
48. T. L. Riss, R. A. Moravec, A. L. Niles, S. Duellman, H. A. Benink, T. J. Worzella and L. Minor, *Cell viability assays guidance manual [Internet]*. Eli Lilly & Company and the National Centre for Advancing Translational Sciences, Bethesda (MD) (2016).
49. G. Ramage, K. V. Walle, B. L. Wickes and J. L. Lopez-Ribot, *J. Clin. Microbiol*., **39**, 3234 (2001).
50. Y. Jin, H. K. Yip, Y. H. Samaranayake, J. Y. Yau and L. P. Samaranayake, *J. Clin. Microbiol*., **4**, 2961 (2003).
51. B. J. Xavier and R. K. Foster, *PNAS*, **104**, 876 (2007).
52. J. E. Nett, M. T. Cain, K. Crawford and D. R. Andes, *J. Clin. Microbiol*., **49**, 1426 (2011).
53. D. Cavalieri, M. Di Paola, L. Rizzetto, N. Tocci, C. De Filippo, P. Lionetti, A. Ardizzoni, B. Colombar, S. Paulone, I. G. Gut, L. Berna, M. Gut, J. Blanc, M. Kapushesky, E. Pericolini, E. Blasi and S. Peppoloni, *Front. Immunol*., **8**, 1997 (2018).
54. J. L. Brown, C. Delaney, B. Short, M. C. Butcher, E. Mckloud, C. Williams, R. Kean and G. Ramage, *mSphere*, **5**, e00371-20 (2020).
55. R. Kean, C. Delaney, R. Rajendran, L. Sherry, R. Metcalfe, R. Thomas, W. McLean, C. Williams and G. Ramage, *J. Fungi*, **4**, 12 (2018).